Analytical Methods

ROYAL SOCIETY OF CHEMISTRY

PAPER

View Article Online
View Journal

Cite this: DOI: 10.1039/d5ay02102b

Development of an effective preconcentration strategy for the trace determination of nickel in thyme tea extracts by $FeSbO_4$ nanoparticle-based dispersive solid phase extraction (DSPE)

Muhammed Ali Büyük, [ab] Hakan Serbest [*c] and Sezgin Bakırdere [*ad]

In the present study, an accurate, rapid and green analytical method based on $FeSbO_4$ nanoparticle-assisted dispersive solid phase extraction (DSPE) was developed to determine trace levels of nickel (Ni) by flame atomic absorption spectrophotometry (FAAS). The fabrication of the $FeSbO_4$ nanoparticles was achieved under hydrothermal synthesis conditions and utilized for the first time as sorbent materials for the preconcentration/separation of Ni ions. A univariate optimization approach was applied to determine the optimal conditions for the extraction parameters. Under the optimal conditions, the limit of detection and the dynamic linear range were found to be 0.81 μg L^{-1} and between 4.0 and 40 μg L^{-1}, respectively. The sensitivity of FAAS was improved by 137.8-fold. Thyme tea samples were spiked to assess the applicability of $FeSbO_4$-DSPE-FAAS, and the percent recovery results between 84.8% and 120.6% obtained with the matrix matching calibration strategy demonstrated that the developed method is feasible for determining nickel ions in thyme tea and similar matrices with high accuracy. The Eco-Scale index was evaluated to determine the greenness of the developed preconcentration protocol, and a net score of 88 was calculated, indicating excellent environmental characteristics.

Received 19th December 2025
Accepted 20th March 2026

DOI: 10.1039/d5ay02102b

rsc.li/methods

1. Introduction

Nickel and its alloys, which have been frequently employed by human beings since ancient times, have historical traces in many areas, such as defense equipment, daily tools, and artistic objects.[1] Currently, nickel is one of the primary metals utilized in the electroplating industry.[2] The presence of nickel in direct contact with humans is a health concern. Chronic exposure to nickel and its salts results in serious health problems such as allergy, cancer, cardiovascular, respiratory and kidney diseases.[3] On the other hand, it has been reported that prolonged contact of the skin with metallic nickel and its alloys causes deformation of the stratum corneum layer, resulting in a special type of eczema called nickel eczema. Although this dermatological disease was previously only an occupational disease in workers in industries working with nickel, it has also been observed in people outside the industry due to their chronic contact with nickel-containing items in daily life.[4] In the findings related to nickel allergy, a prevalence rate of 9.8% was observed among Swedish women aged 16–19 between 2011 and 2013, while a prevalence rate of 14–18% was observed among adults of both genders in other European Union countries between 2008 and 2011. Additionally, in 2012, a prevalence of approximately 11.6% was reported among girls undergoing patch testing due to suspected allergic contact dermatitis in Germany, Austria, and Switzerland.[5] Nickel and its compounds, which are found naturally in the Earth's crust, are released into the environment through several human activities such as refining, smelting, mining, metal industry applications, and waste and fossil fuel combustion and through natural sources such as meteoric dust, volcanic eruptions, windblown dust and forest fires. Considering that nickel emissions to the atmosphere from natural sources were 30 million kg per year in the early 1990s, the exposure of the world population to low levels of nickel through inhalation, water and food is of great concern for human health and environmental resources.[3,6] In particular, nickel, which is transferred to the roots, stems or leaves of plants consumed as food, enters the metabolism through digestion.[7] Although the European Food Safety Authority (EFSA) has set a tolerance limit of 2.8 μg kg^{-1} of nickel per body weight, World Health Organization (WHO) guidelines have reported nickel concentrations between 0.01 and 0.10 mg kg^{-1} in different foods. For this reason, it is essential to monitor nickel levels with high accuracy, especially in food matrices.[8] The release from materials

[a]Yildiz Technical University, Faculty of Arts and Sciences, Department of Chemistry, 34220 İstanbul, Turkiye. E-mail: bsezgin23@yahoo.com
[b]Yildiz Technical University, Faculty of Chemistry and Metallurgy, Department of Chemical Engineering, 34220 İstanbul, Turkiye
[c]Mimar Sinan Fine Arts University, School of Conservation and Restoration of Cultural Property, 34380 İstanbul, Turkiye. E-mail: hakan.serbest@msgsu.edu.tr
[d]Turkish Academy of Sciences (TÜBA), Vedat Dalokay Street, No: 112, Çankaya, 06670, Ankara, Turkiye

used for brewing tools is a possible source of nickel contamination in food and water matrices.[9] According to current data, the WHO has set the legal limit for Ni in drinking water to 70 μg L^{-1}. However, a study in the literature reported that Ni concentrations after tea infusion in traditional metallic and stainless–steel teapots ranged from 41 to 209 μg L^{-1}, and in one sample, it was 856 μg L^{-1}. When Pyrex glass pots were used for infusing, the mean nickel concentration was found to be 32 μg L^{-1}.[10] These levels are believed to be due to the release from the teapot and the tea content. Spices have been used in foods for a very long time due to their flavor enhancing properties. Among them, thyme is a spice with pharmacological properties that is commonly used to enhance the flavor of food. Thymol and carvacrol, as the two main constituents of thyme, exhibit antioxidant, anti-inflammatory and neurologically beneficial effects that support the widespread use of thyme.[11] Garden thyme, named *Thymus vulgaris* in the Lamiaceae family, is widely grown for brewing tea in the Mediterranean region.[12] More than 450 plant species worldwide have been proven to exhibit hyperaccumulatory effects and retain heavy metals in their structures. The most hyperaccumulatory effect, especially in green leafy plants, is associated with nickel. Of these, some Mediterranean plants have been reported to be nickel hyperaccumulators.[13] According to a declaration issued at the North Atlantic Treaty Organization (NATO) conference in 1983, a high concentration of nickel was detected in a large part of the Mediterranean Sea.[14] Therefore, one of the main reasons for nickel accumulation might be linked to the increased nickel concentration in water, an essential soil requirement, in the Mediterranean region. Hence, the determination of trace nickel levels in thyme samples with high accuracy is an important issue for analytical research in food safety.

In the literature, analytical techniques frequently employed for nickel determination are inductively coupled plasma-optical emission spectrometry (ICP-OES),[15] inductively coupled plasma-mass spectrometry (ICP-MS),[16] graphite furnace atomic absorption spectrometry (GFAAS),[17] atomic fluorescence spectrometry,[18] anodic stripping voltammetry[19] and flame atomic absorption spectrometry (FAAS) analyses.[8] FAAS, which can be applied to 68 elements in the concentration range of mg L^{-1} in various matrices, is one of the basic spectroscopic techniques widely utilized in many laboratories, with the advantages of relatively low operator skill, low cost and easy operation for routine analysis.[20] The high cost and difficulty of accessibility of systems such as ICP-OES and ICP-MS, as well as the cost, matrix modifier, and temperature program requirements of the GFAAS system, are significant limitations in practice.[21,22] On the other hand, the disadvantages of FAAS include low sampling efficiency as a result of the low nebulization system and poor sensitivity due to the very short residence time of atoms in the light path. Hence, the implementation of an appropriate sample preparation procedure allows for sensitive and accurate analyte determinations.[23]

For this goal, various extraction methods have been presented for the preconcentration and separation of nickel from complex matrices, such as dispersive liquid–liquid microextraction (DLLME),[24] cloud point extraction (CPE),[25] solidified floating organic drop formation microextraction (SFODFME)[26] and dispersive solid phase extraction (DSPE).[27] The DSPE method, based on the principle that the sorbent material adsorbs the analyte(s) on its surface by dispersing in the sample solution, minimizes the drawbacks of the traditional SPE method, such as long equilibration time and poor extraction yield.[28] On the other hand, thanks to the significant advances in nanotechnology in recent years, the idea of utilizing nanoparticles fabricated for different purposes as sorbent materials has made the DSPE method more attractive. For this reason, numerous sorbent materials with different physical and chemical properties have appeared in various analytical applications. Nanoparticles (NPs), with at least one dimension smaller than 100 nm, are innovative materials made of inorganic and organic compounds with high porosity, minimal size and active adsorption sites that are capable of adsorbing a variety of pollutants.[29,30]

The materials with the ABO_4-type structures have been the topic of different studies in various engineering applications, such as Li-ion batteries, gas sensors, photocatalysts, photodetector systems, and solar energy transformations.[31] Among these materials, iron antimonate ($FeSbO_4$), a Sb mineral also known as tripuhyite, has been reported to be employed as an important catalytic material for the selective oxidation of hydrocarbons.[32,33] It has been indicated that $FeSbO_4$ particles have a broad surface area thanks to their nanoscale dimensions when the morphological structure was analyzed.[33] Moreover, it has been reported that two or more mixed metal oxides exhibit better performance in adsorption-based processes than single metal oxides, such as Fe_3O_4, TiO_2, and SnO_2, and binary metal oxides, such as M_xO_y/M_zO_t, due to their synergistic enhancement properties.[34] Metal organic frameworks (MOFs), despite being innovative materials, exhibit low stability in aqueous environments and poor degradability, indicating the adequacy of metal oxides in this context.[35] As a result, a mixed metal oxide nanoparticle such as $FeSbO_4$ has the potential to be utilized as a sorbent material in various studies due to its characteristics, such as its high surface area and chemical stability.

In light of this background, it has been suggested that $FeSbO_4$ could be used as a sorbent material for a preconcentration/separation study. Accordingly, since no previous studies using $FeSbO_4$ have been found in the literature, $FeSbO_4$ was used for the first time as a sorbent material for the preconcentration of a hyperaccumulative inorganic analyte such as nickel in thyme tea matrices. Since it is known that Sb-enriched regions on the $FeSbO_4$ surface contain more active sites,[36] the effect of mixed metal oxide nanoparticles, such as $FeSbO_4$, on the efficiency of Ni(II) ion preconcentration/separation was evaluated through the sensitivities of FAAS and improved FAAS systems. Developing a $FeSbO_4$-DSPE-FAAS method for the accurate determination of Ni at trace levels with high sensitivity will provide a good alternative method for the evaluation of Ni levels in different matrices to check the legal tolerable limit of Ni.

2. Materials and methods

2.1. Reagents and chemicals

Analytical grade chemicals and reagents were employed throughout the experiments. Deionized water with

a conductivity of 18.2 MΩ cm was supplied by an Elga Purelab Flex 3 Water System (High Wycombe, United Kingdom) for the preparation of standard and sample solutions and washing of experimental materials. The nickel standard solutions at different concentrations were produced by diluting 1000 mg kg^{-1} of nickel(II) stock solution prepared by dissolving nickel(II) nitrate hexahydrate (Carlo Erba, Spain) in 0.02% of nitric acid (Merck, Germany) to lower concentrations. Antimony(III) chloride ($SbCl_3$) (>99%) and iron(III) nitrate nonahydrate ($Fe(NO_3)_3 \cdot 9H_2O$) (>99%) salts used for the synthesis of $FeSbO_4$ NPs were purchased from Sigma-Aldrich (USA) and Merck (Germany), respectively. Ethanol (96%) (Tekkim, Türkiye) was utilized to remove possible impurities on the surface of the synthesized nanoparticles. Buffer solutions were prepared using 0.40 M of potassium hydrogen phthalate (Merck, Germany) for pH 4.0, 5.0 and 6.0, 0.90 M of hydroxymethyl aminomethane (tris) (Merck, Germany) for pH 7.0 and 0.12 M of sodium tetraborate decahydrate (Sigma-Aldrich, Germany) for pH 8.0, 9.0 and 10, respectively.

Hydrochloric acid (HCl) (37%) and sodium hydroxide (NaOH) were bought from Merck (Germany) to adjust the pH of the solutions. Acetylene supplied by a local vendor in İstanbul, Türkiye was used for the fuel fed to the atomizer unit. Thyme samples utilized for the recovery studies were purchased from packaged products of different brands in supermarkets in İstanbul, Türkiye.

2.2. Apparatus

The quantitative and qualitative determination of nickel were performed using an atomic absorption spectrophotometer (FAAS) model ATI UNICAM AA929 integrated with a deuterium (D_2) lamp for background correction. The spectroscopic measurements were achieved using a Varian brand nickel hollow cathode lamp producing light at a wavelength of 232.0 nm and a slit width of 0.50 nm. $FeSbO_4$ nanoparticles were synthesized in a Nuve FN120 oven (Türkiye). A Mettler Toledo (USA) S220-K Seven Compact benchtop pH/ion meter equipped with an InLab Expert electrode was employed to control the pH of the solutions. After synthesis, a Heraeus oven was used to dry $FeSbO_4$ nanoparticles. An MRC-Clean01 model ultrasonic bath, an Isolab-M101002 model vortex mixer (Germany) and a Heidolph (Germany) mechanical stirrer were used to ensure the effective homogenization of the solutions/samples. Phase separation was carried out using a Biobase BKC TL5II (China) model centrifuge system. A four-stage Shimadzu (Japan) ATX224R precision balance was used to weigh the solid materials.

2.3. Synthesis and characterization of $FeSbO_4$ nanoparticles

The synthesis of $FeSbO_4$ NPs was established by modifying the procedure of a study in the literature.[33] Accordingly, 5.0 mmol of antimony(III) chloride and iron(III) nitrate nonahydrate were weighed and transferred to different beakers. Due to the known low solubility of antimony compounds in water,[37] 5.0 mL of 10 M nitric acid was used to dissolve antimony(III) chloride. Iron(III) nitrate nonahydrate, a water-soluble compound, was dissolved directly in 5.0 mL of distilled water. After dissolving the salts, the obtained solutions were mixed with each other. Then, 10 M of NaOH was added dropwise until the pH of the mixture reached the range of 9.5–10.0, and stirring continued using a magnetic stirrer for about 25 minutes until the solution color turned to brick. After the mixture was diluted with deionized water to a final volume of 30 mL, it was transferred to a Teflon container. The synthesis of nano-sized and homogeneous $FeSbO_4$ particles was carried out in an autoclave at 160 °C for 12 hours. After the synthesis reaction was completed, centrifugation was applied to ensure phase separation, and the fabricated $FeSbO_4$ NPs were washed several times with deionized water and ethanol to remove possible impurities and then dried in an oven set at 50 °C for 24 hours. Subsequently, the calcination process was carried out at 600 °C for 4.0 hours to obtain the high purity of $FeSbO_4$ NPs.

2.4. Preparation of real samples

In this study, thyme tea, one of the spice teas frequently consumed in daily life due to its several claimed benefits, was selected as the real sample. Thyme samples were purchased from two brands from a herbalist in İstanbul, Türkiye. The infusion process for each thyme sample was performed by brewing 1.0 g of each thyme in 200 mL of boiled drinking water for 20 minutes. Subsequently, filtration was carried out using filter paper to separate the thyme pulp from the liquid phase, and the samples were diluted. Then, the spiking processes were carried out at final Ni concentrations of 10, 15, 20 and 25 μg L^{-1} in the thyme tea samples.

2.5. Procedure for the $FeSbO_4$-DSPE-FAAS method

The developed extraction procedure includes the adsorption of Ni(II) ions in the sample solution with the help of NPs by applying a mixing process and the release of Ni(II) ions from the NP surface by adding an eluent after phase separation. Briefly, 20 mg of $FeSbO_4$ NPs and 1.0 mL of pH 7.0 buffer were added to 40 mL of the sample solution. Then, vortexing was performed for 60 s to ensure an efficient interaction between Ni(II) and $FeSbO_4$ NPs. The sorbent and liquid phases were separated from each other by centrifugation, and the supernatant was decanted. To release the Ni(II) ions transferred to the $FeSbO_4$ surface, 100 μL of 1.0 M nitric acid was added. After phase separation, the extraction phase was fed to the FAAS system, and measurements were carried out.

3. Results and discussion

Optimization studies were carried out using a univariate optimization approach to determine the optimum experimental conditions for the main parameters affecting nickel extraction efficiency, such as pH, sample volume, buffer solution volume, sorbent amount, eluent volume/concentration and vortexing time, with three replicate measurements and to improve the detection power of the FAAS system. In this context, the working ranges of variables were determined as follows: 4.0–9.0 for pH, 10–40 mL for sample volume, 1.0–2.5 mL for buffer solution

volume, 5.0–40 mg for sorbent, 0.50–14.33 M for eluent concentration, 75–200 μL for eluent volume, vortex, orbital shaker and ultrasonication for mixing type and 15–90 s for vortexing.

3.1. Characterization studies

The characterization studies were achieved by scanning electron microscopy (SEM), energy-dispersive X-ray spectroscopy (EDX) and X-ray diffraction (XRD) techniques to investigate the morphological and crystalline structures of $FeSbO_4$ NPs. The SEM image shown in Fig. 1a revealed that $FeSbO_4$ particles are nanosized and have a very large surface area. The EDX quantitative analysis shown in Fig. 1b demonstrated that the elements Fe (24.95 wt%), Sb (48.82 wt%), and O (26.23 wt%) are predominant, in accordance with the $FeSbO_4$ structure. The XRD patterns presented in Fig. 1c were obtained at a radiation generation setting of 40 mA and 45 kV by scanning in the angular range of 2.0–90° of 2θ with a step size of 0.013°. The responses recorded against 2θ angles were in accordance with the characteristic peaks described for $FeSbO_4$ in comparison with the literature findings.[38–40] Moreover, in the study used as the reference for the synthesis procedure,[33] it was noted that the characteristic $FeSbO_4$ patterns became more prominent with increasing calcination temperature, supporting that the XRD patterns presented in Fig. 1c correspond to the $FeSbO_4$ structure.

3.2. Impact of pH and buffer volume

In adsorption-based preconcentration/separation studies, the pH of the sample solution has a primary influence on the surface charge of the adsorbent and the predominant form of the analyte(s).[41] Moreover, as the pH of the medium approaches the acidic region, the concentration of H_3O^+ ions in the medium increases; competition occurs with a certain amount of analyte ions for active adsorption sites of the sorbent, and the ability of target analytes to bind to the sorbent is significantly affected.[42] In light of these findings, different pH values between 4.0 and 9.0 were tested to determine the optimum pH of the sample solution. According to the results shown in Fig. 2, the mean absorbance values showed a linear increase from pH 4.0 to pH

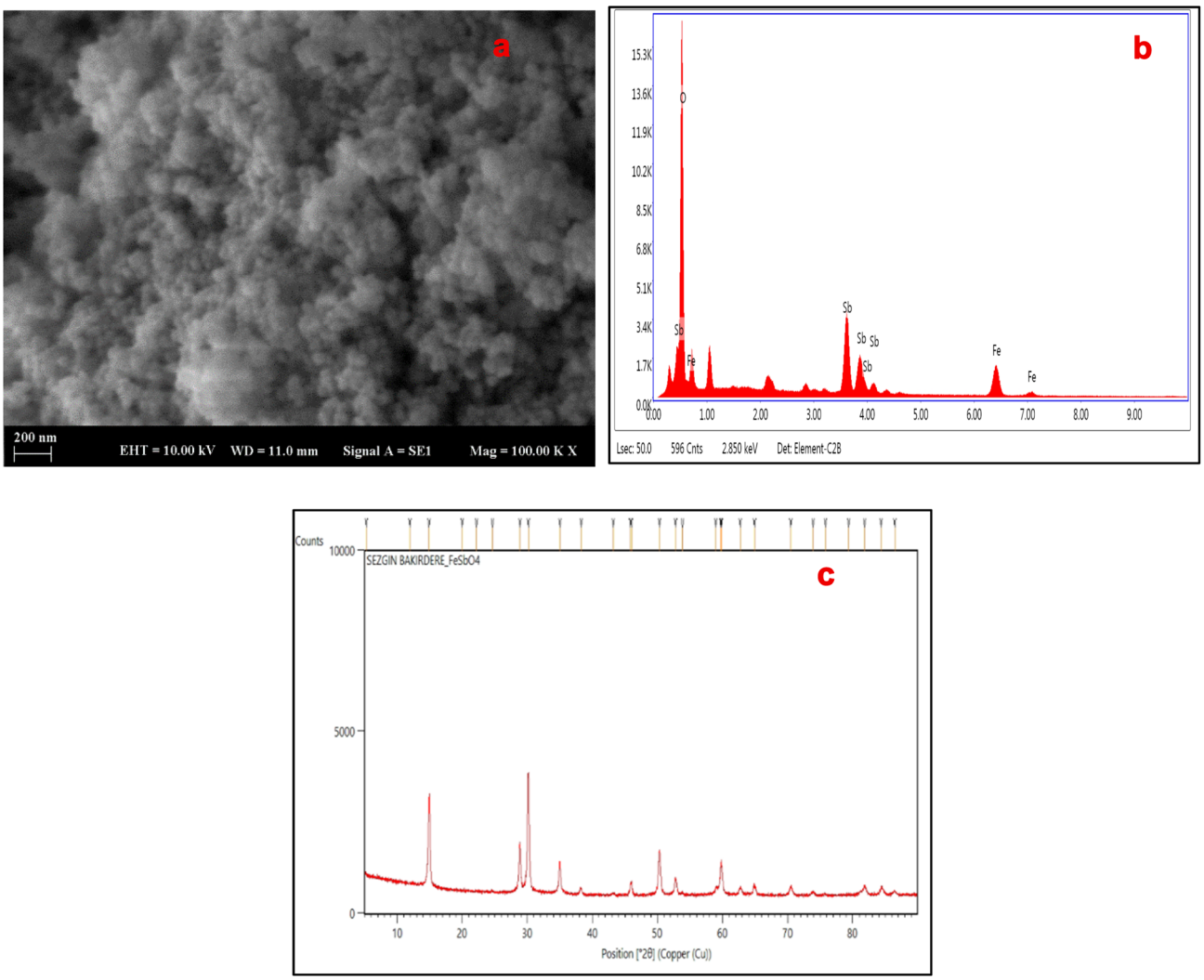

Fig. 1 (a) SEM image of $FeSbO_4$ NPs. (b) EDX image of $FeSbO_4$ NPs. (c) XRD pattern of $FeSbO_4$ NPs.

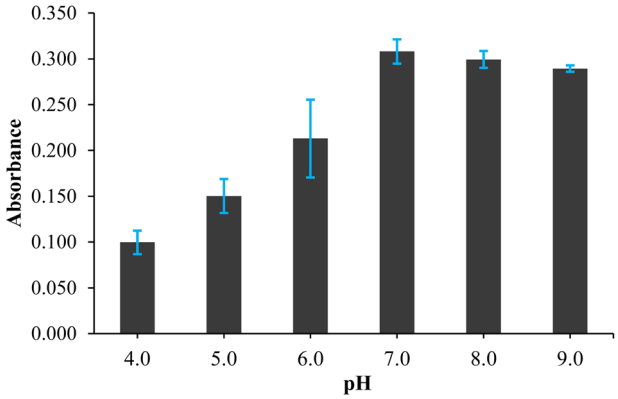

Fig. 2 Impact of pH on the microextraction efficiency. (Experimental conditions: 20 mL of 0.10 mg L^{-1} Ni(II), 1.0 mL of buffer solutions, 15 mg of $FeSbO_4$, 30 s of vortexing, and 200 μL of concentrated HNO_3).

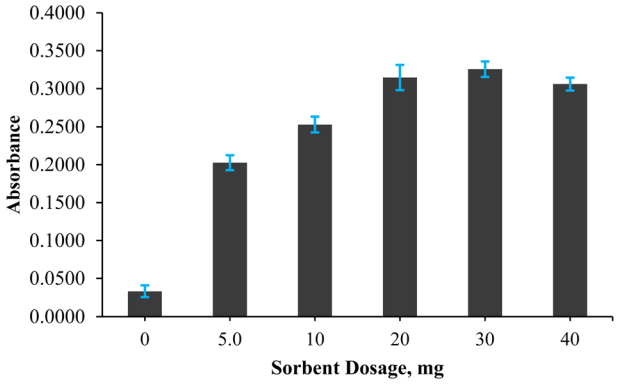

Fig. 3 Impact of $FeSbO_4$ amount on the microextraction efficiency. (Experimental conditions: 20 mL of 100 μg L^{-1} Ni(II), 1.0 mL of pH 7.0, 30 s of vortexing, and 200 μL of concentrated HNO_3).

7.0, reached the highest value at pH 7.0 and decreased slightly from pH 7.0 to pH 9.0. The increase in the mean absorbance values from the acidic to the neutral and alkaline regions is related to the decrease in the presence of protons in the medium. Hence, the optimum pH was selected as 7.0 for further experiments. In the literature, Jalbani and Soylak combined DSPE and ionic liquid-dispersive liquid microextraction to determine Ni in chicken, fish and meat samples and reported a high extraction efficiency for pH 7.0.[43] Hameed reported that in the deep eutectic solvent (DES)-based DLLME method developed to determine trace levels of Ni(II) in different environmental samples, H_3O^+ ions are located to DES functional groups in the acidic region, while in the alkaline region, the extraction efficiency decreases due to the precipitation of nickel in the hydroxyl form, so the optimum solution acidity was recorded for pH 7.0.[44]

Determination of the optimum buffer volume is important both to ensure the pH stability of the solution and to prevent the use of excess chemicals. For this purpose, a pH 7.0 buffer was tested between 1.0 and 2.5 mL under equal conditions. The mean absorbance values decreased after 1.0 mL. The main reason for the decrease in extraction efficiency is that the dilution occurred when more than the required buffer was added to the sample. Therefore, 1.0 mL was determined as the optimal buffer volume.

3.3. Impact of sorbent amount

Determination of the amount of the sorbent material in the extraction procedure is very important in terms of extraction outputs and compliance with the principle of green chemistry. Here, insufficient sorbent amounts result in lower recoveries and extraction efficiencies due to overloading of the analyte ion.[45] On the other hand, an excessive amount of sorbent leads to higher operating costs and waste management processes.[46] Therefore, 5.0, 10, 20, 30 and 40 mg of $FeSbO_4$ were tested under equal conditions. The mean absorbance values depicted in Fig. 3 increased linearly from 5.0 mg to 20 mg, and close results were recorded for 20, 30 and 40 mg of $FeSbO_4$. In addition, to investigate whether nickel precipitates in the hydroxyl form under the given conditions, the experiments were carried out without the addition of nanoparticles, and it was determined by absorbance-based evaluation that nickel precipitated approximately 5.0% in the hydroxyl form. Considering the high adsorption efficiency, cost and solvent consumption for desorption under the given experimental conditions, 20 mg of $FeSbO_4$ was chosen as the optimum sorbent mass.

3.4. Impact of mixing type and period

The mixing process is very crucial to increase the interaction of the components in a mixture/solution and to ensure homogeneity. Associated with the DSPE study, the enrichment of the interaction between the sorbent and analyte(s) is achieved by the application of a mixing process. For this purpose, the highest extraction efficiency was investigated with the help of laboratory-scale instruments, such as vortex, orbital stirrer and ultrasonication. The extraction outputs of these methods were compared to the extraction output without mixing, as shown in Fig. 4. It was found that the mixing process contributed more than 10% to the extraction efficiency and that vortex was the optimum mixing type with high repeatability.

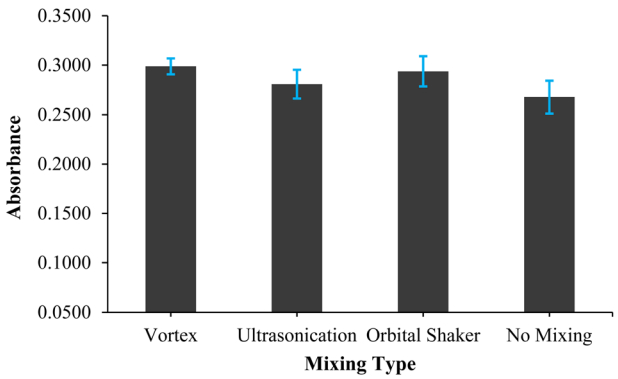

Fig. 4 Impact of mixing time on the microextraction efficiency. (Experimental conditions: 20 mL of 100 μg L^{-1} Ni(II), 1.0 mL of pH 7.0, 20 mg of $FeSbO_4$, and 200 μL of concentrated HNO_3).

The optimization of the mixing period is crucial to determine high extraction efficiency as well as operating cost, applicability and time spent on a sample. To achieve this goal, various vortexing times between 15 and 90 s were tested to determine the optimum mixing period. The obtained mean absorbance values were close to each other, but the highest repeatability was recorded for 60 s with 0.60% RSD. Hence, 60 s was chosen as the optimum vortexing period.

3.5. Impact of eluent concentration and volume

The elution process, also known as desorption, plays a major role in the extraction process to release the analyte(s) settled on the sorbent surface from the sample medium and to evaluate the extraction efficiency. In the literature, it has been reported that the concentration and volume of the eluent, as well as the type of eluent, are very important parameters in the achievement of effective desorption efficiency and high enrichment factors.[47] Acid solutions are frequently used in the desorption process due to their ability to generate protonation on the surface of the sorbent material. Of these, nitric acid is suitable for spectroscopic measurements and is an effective solvent for the release of metal analyte(s) from the sorbent surface. First, HNO_3 concentrations between 0.50 and 14.33 M were tested to determine the ability to release Ni(II) ions from the $FeSbO_4$ surface with high efficiency. In the recorded results, the mean absorbance values were very close to each other for 0.50 and 5.0 M and showed a decrease for 14.33 M. A high acid concentration leads to poor nebulization for the atomization unit due to increased viscosity, which has a direct influence on the measurement results. On the other hand, the optimum HNO_3 concentration of 1.0 M was selected to ensure effective desorption in real sample applications.

The eluent volume plays a significant role as the final volume in determining the enrichment factor. The critical point here is that excessive usage of the desorption solution leads to dilution of the analyte(s), while insufficient volume leads to the failure to release analyte ions from the surface with high efficiency. The extraction process was performed under equal conditions to determine the optimal eluent volume by adding different volumes of 1.0 M HNO_3 between 75 and 200 μL. As illustrated in Fig. 5, the highest mean absorbance value was obtained for 75 μL, and a linear decrease was recorded from 75 μL to 200 μL. The repeatability of the measurement for 75 μL was poor for confident results. Here, it is considered that although sufficient feed volume was provided for the FAAS system, it is considered that 75 μL is not adequate for the desorption of Ni(II) from the $FeSbO_4$ NP surface for repeatable results. Hence, 100 μL was chosen as the optimum eluent/desorption volume.

3.6. Impact of sample volume

In the extraction process, the initial and final volume ratios theoretically provide the preconcentration factor. Therefore, the sample volume, which can be defined as the initial volume, directly affects the extraction efficiency.[48] For this purpose, the extraction process was carried out under equal conditions for different sample volumes between 10 and 40 mL in 10 mL increments. In the results shown in Fig. 6, the mean absorbance values increased linearly from 10 mL to 40 mL, and the highest extraction efficiency was obtained for 40 mL. Considering the volume of the sample tube, volumes above 40 mL were not attempted, as effective mixing could not be achieved. Therefore, 40 mL was determined as the optimum sample volume for the developed DSPE-FAAS approach.

The summarized optimum conditions belonging to DSPE-FAAS are illustrated in Table 1.

3.7. Assessment of the system analytical performance

Subsequent to the optimization experiments, the analytical performance values of the developed system, including the limit of detection (LOD)/quantification (LOQ) and linear working range coefficient of integration (R^2), were evaluated under the optimum experimental conditions, as illustrated in Table 1. The standard deviation of 6 replicates of the lowest concentration in the linear operating range and the slope of the calibration plot equation were utilized to calculate LOD and LOQ. Accordingly, LOD and LOQ values were calculated as 3 and 10 times the ratio of the standard deviation to the slope, respectively, and were found to be 0.81 and 2.7 μg L^{-1}, respectively. The linear

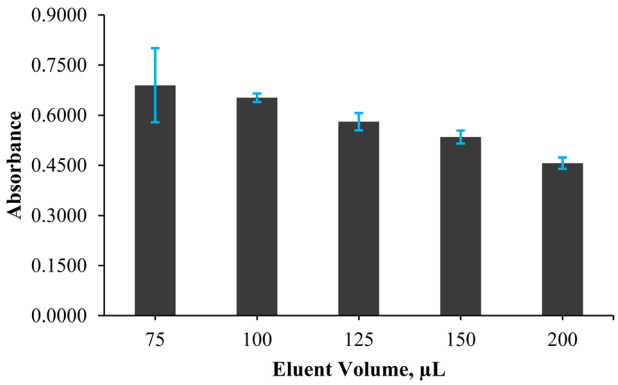

Fig. 5 Impact of eluent volume on the microextraction efficiency. (Experimental conditions: 20 mL of 100 μg L^{-1} Ni(II), 1.0 mL of pH 7.0 buffer solution, 20 mg of $FeSbO_4$, and 45 s of vortexing).

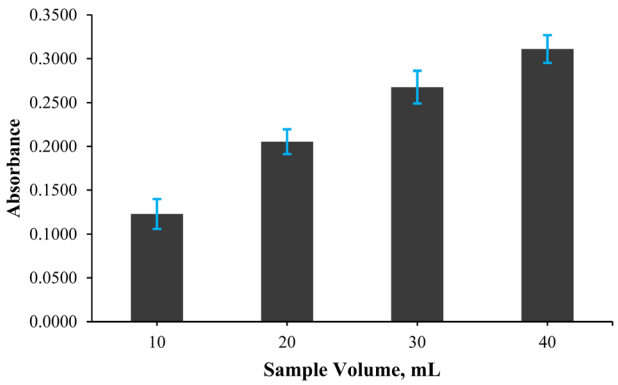

Fig. 6 Impact of sample volume on the microextraction efficiency. (Experimental conditions: 1.0 mL of pH 7.0 buffer solution, 20 mg of $FeSbO_4$, 60 s of vortexing, and 100 μL of 1.0 M HNO_3).

Table 1 Optimal conditions for the DSPE-FAAS strategy in the preconcentration of nickel

Experimental parameters	Optimum condition
pH and buffer volume	pH 7.0/1.0 mL
Sample volume	40 mL
Mass of $FeSbO_4$	20 mg
Vortexing duration	60 s
Eluent concentration and volume	1.0 M of HNO_3/100 μL

calibration range was determined to be between 4.0 and 40 μg L^{-1}, and R^2 was 0.9934. The method achieved a good relative standard deviation (%RSD) of 3.3% for 4.0 μg L^{-1}, 5.3% for 10 μg L^{-1} and 5.1% for 30 μg L^{-1}. On the other hand, no analytical signal belonging to the analyte was observed in the blank analyses performed; only baseline noise was present. The linear calibration plot equations for the FAAS and $FeSbO_4$-SPME-FAAS systems were presented as $y = 0.0475x + 0.0329$ and $y = 6.547x + 0.0353$, respectively, with a concentration based on mg L^{-1}. When the slope values were compared, the increase in sensitivity was calculated to be 137.8-fold. The analytical figures of these two systems are summarized in Table 2.

3.8. Comparison with other reported preconcentration methods for nickel determination

Different research groups have previously conducted various studies to determine trace levels of nickel, whose detrimental effects on human health and the environment have been reported in many studies. In 2024, Soylak *et al.* complexed Ni(II) ions with 2-(5-bromo-2-pyridylazo)-5-diethylamino-phenol, followed by a 10-fold enhancement using activated nanodiamonds@Bi_2WO_6 nanocomposite and recorded a LOD of 1.6 μg L^{-1} in UV-vis.[27] In 2015, Wang *et al.* reported a 79-fold enhancement factor for the determination of trace levels of Ni(II) in food and environmental water samples by complexing with diethyldithiocarbamate and separating it with Fe_3O_4.[49] In the method proposed by Topuz in 2020 for the determination of Ni(II) in environmental and pharmaceutical samples, Ni(II) and 2,6-dimethyl-morpholinedithiocarbamate ligands were complexed; then, Ni(II) was preconcentrated 20-fold with 200 mg of Amberlite XAD-4 sorbent.[50] In 2019, Kojidi and Aliakbar developed a preconcentration method to determine Ni(II) at trace levels in natural water and wastewater samples. Ni(II) ions complexed with poly(*p*-aminophenol) were separated from the matrix with 150 mg graphene oxide and enhanced 67-fold.[51] In 2023, Ahmed and Soylak synthesized the magnetic luffa@MOF-199 sorbent to develop the DSPE method for the removal of Ni(II) ions from various food and water samples. The removal protocol using 20 mg of sorbent resulted in a 48.7-fold improvement in detection power.[52] As can be observed from the results summarized in Table 3, the developed $FeSbO_4$-DSPE-FAAS stands out with its features that simplify the extraction steps and separate Ni(II) ions from the complex matrix in high yields without any chelation. The LOD values vary depending on the systems used, but when enrichment factors are considered, the 137.8-fold enhancement of Ni(II) by $FeSbO_4$-DSPE-FAAS makes the method attractive. Moreover, additional experiments by applying the extraction protocol under the same conditions show that the $FeSbO_4$ nanoparticles may be utilized at least twice without any structural changes.

3.9. Recovery studies

Recovery studies are an essential step in assessing the feasibility of the developed analytical method. The measurements performed on real samples at different concentrations after applying the method steps enabled the correlation and evaluation between the added and determined concentrations. The applicability of this method was assessed using samples of thyme tea, which is frequently consumed by people daily. For this purpose, the thyme tea samples whose preparation procedure is described in the "Preparation of Real Samples" section

Table 2 Calculated system analytical performance values of the FAAS and $FeSbO_4$-DSPE-FAAS methods

Method	LOD, μg L^{-1}	LOQ, μg L^{-1}	R^2	Linear range, μg L^{-1}	Equation	Enhancement in sensitivity
FAAS	187.2	624.0	0.9917	400–5000	$y = 0.0475x + 0.0329$	—
$FeSbO_4$-DSPE-FAAS	0.81	2.7	0.9934	4.0–40	$y = 6.547x + 0.0353$	137.8

Table 3 Literature findings for determining nickel in trace levels

Sorbent	System	LOD, μg L^{-1}	pH	Sorbent amount, mg	PF*	Related study
Activated nanodiamonds@Bi_2WO_6	UV-vis	1.6	6.0	20	10	27
Fe_3O_4	ICP-MS	0.009	8.0	30	79	49
Amberlite XAD-4	UV-vis	1.37	5.0	200	20	50
Graphene oxide	UV-vis	0.70	7.0	150	67	51
Magnetic luffa@metal-organic frameworks (MOF-199)	FAAS	0.35	7.0	20	48.7	52
$FeSbO_4$	FAAS	0.81	7.0	20	137.8	This work

Table 4 Percentage recovery results calculated for thyme tea matrices ($n = 4$)[a]

	Spiking concentration, μg L^{-1}	Mtx. mth. cal. recovery ± SD, %
SAMPLE A	Blank	Not detected
	10	93.4 ± 6.6
	15	120.6 ± 1.5
	20	107.9 ± 11.5
	25	118.4 ± 18.0
SAMPLE B	Blank	Not detected
	10	109.1 ± 12.0
	15	88.6 ± 6.9
	20	84.8 ± 8.3
	25	91.2 ± 4.1

[a] SD: standard deviation and Mtx. Mth. Cal.: matrix matching calibration.

were spiked to final concentrations of 10, 15, 20 and 25 μg L^{-1}. Then, the extraction protocol was applied to both tea samples, and the results of the spectroscopic measurements were first evaluated according to the external calibration plot equation. It was determined that the different components in thyme tea suppress analytical signals and therefore cause negative interference effects. Therefore, the matrix matching calibration method was applied to improve the accuracy and reliability of the measurement results by minimizing matrix-associated interference effects. For this purpose, the calibration plot equation obtained for each sample was used to calculate the percent recovery results from the absorbance values of different concentrations of the other samples. The good recovery results between 84.8% and 120.6% demonstrated the applicability of the developed $FeSbO_4$-DSPE-FAAS method for thyme tea samples. The summarized recovery results are shown in Table 4.

3.10. Greenness evaluation of the developed method

The investigation of the applicability of an analytical method developed with a focus on green chemistry is as essential as achieving the main aims of the study. More than 20 years ago, Anastas and Warner introduced twelve fundamental green chemistry principles that adopt a broader view of chemical processes to ensure sustainability in the protection of human health and environmental resources.[53] Along with the development of technology, different evaluation tools have been developed to assess the "green" characteristics of the reported methods. In the "Eco-Scale" method introduced by Galuszka *et al.* in 2012, an assessment is carried out on the environmental friendliness of the relevant experimental procedures by assigning penalty points based on the type and amount of chemicals and reagents, the instruments, and the amount of waste generated. Then, the net score is calculated by subtracting the total penalty points from the initial 100 points and is presented with the corresponding environmental equivalent.[54] In this context, 40 mL of sample, 1.0 mL of buffer solution, 0.10 mL of 1.0 M HNO_3, FAAS, acetylene, and <1.0 mL (g) waste generation parameters were assigned penalty points of 2, 1, 4, 1, 3, and 1, respectively, resulting in a total of 12 penalty points and a greenness score of 88. Since this result was >75, it was presented as an "excellent green method".

4. Conclusion

A green-friendly, fast and effective method ($FeSbO_4$-DSPE-FAAS) for the determination of trace levels of nickel is presented in this study. $FeSbO_4$ was synthesized in nanoscale form by hydrothermal synthesis under laboratory conditions and utilized as a sorbent material for the separation/preconcentration of nickel ions from the matrix environment. The optimization of the parameters affecting extraction efficiency was achieved univariately, and an LOD of 0.81 μg L^{-1} was calculated under optimal conditions. The increase in sensitivity was found to be 137.8 times by comparing the slopes of the calibration plot equations of the FAAS and $FeSbO_4$-DSPE-FAAS systems. It has been proven that $FeSbO_4$ nanoparticles can be reused at least twice. The compatibility of the developed method with green chemistry principles was investigated using the Eco-Scale tool, and it was recorded as an excellent environmentally friendly method with a greenness score of 88. The spike experiments were carried out to investigate the applicability/accuracy of the method developed in recovery studies on thyme tea samples. The recovery results recorded between 84.8% and 120.6% with the matrix matching calibration strategy supported the idea that the $FeSbO_4$-DSPE-FAAS method can be used for the determination of nickel with high accuracy in thyme tea samples.

Conflicts of interest

The authors declare no conflicts of interest.

Data availability

Data will be made available upon reasonable request.

References

1 F. B. Howard – White, *Nickel*, Routledge, London, 2023.
2 E. C. Gugua, C. O. Ujah, C. O. Asadu, D. V. Von Kallon and B. N. Ekwueme, *Hybrid Adv.*, 2024, **7**, 100286.
3 G. Genchi, A. Carocci, G. Lauria, M. S. Sinicropi and A. Catalano, *Int. Res. J. Publ. Environ. Health*, 2020, **17**, 679.
4 M. G. Ahlström, J. P. Thyssen, M. Wennervaldt, T. Menné and J. D. Johansen, *Contact Dermat.*, 2019, **81**, 227–241.
5 M. G. Ahlström, J. P. Thyssen, T. Menné and J. D. Johansen, *Contact Dermat.*, 2017, **77**, 193–200.
6 W. Begum, S. Rai, S. Banerjee, S. Bhattacharjee, M. H. Mondal, A. Bhattarai and B. Saha, *RSC Adv.*, 2022, **12**, 9139–9153.
7 M. U. Hassan, M. U. Chattha, I. Khan, M. B. Chattha, M. Aamer, M. Nawaz, A. Ali, M. A. U. Khan and T. A. Khan, *Environ. Sci. Pollut. Res.*, 2019, **26**, 12673–12688.
8 B. Kartoğlu, S. Bodur, E. Gülhan Bakırdere and S. Bakırdere, *Microchem. J.*, 2024, **205**, 111349.

9 Z. Liao, Y. Chen, J. T. Tzen, P. Kuo, M. Lee, F. Mai, T. Rairat and C. Chou, *J. Sci. Food Agric.*, 2018, **98**, 751–757.
10 D. Schrenk, M. Bignami, L. Bodin, J. K. Chipman, J. del Mazo, B. Grasl-Kraupp, C. Hogstrand, L. (Ron) Hoogenboom, J. Leblanc, C. S. Nebbia, E. Ntzani, A. Petersen, S. Sand, T. Schwerdtle, C. Vleminckx, H. Wallace, T. Guérin, P. Massanyi, H. Van Loveren, K. Baert, P. Gergelova and E. Nielsen, *EFSA J.*, 2020, **18**(11), 6268.
11 S. Qi, P. Zhan, H. Tian, P. Wang, X. Ma and K. Li, *Food Sci. Hum. Wellness*, 2022, **11**, 305–315.
12 E. Akoury, C. Baroud, S. El Kantar, H. Hassan and L. Karam, *Toxicol. Rep.*, 2022, **9**, 1962–1967.
13 T. Pardo, B. Rodríguez-Garrido, R. F. Saad, J. L. Soto-Vázquez, M. Loureiro-Viñas, Á. Prieto-Fernández, G. Echevarria, E. Benizri and P. S. Kidd, *Sci. Total Environ.*, 2018, **630**, 275–286.
14 A. J. Spivack, S. S. Huested and E. A. Boyle, in *Trace Metals in Sea Water*, Springer, US, Boston, MA, 1983, pp. 505–512.
15 S. L. dos Anjos, J. C. Alves, S. A. Rocha Soares, R. G. O. Araujo, O. M. C. de Oliveira, A. F. S. Queiroz and S. L. C. Ferreira, *Talanta*, 2018, **178**, 842–846.
16 L. Poirier, J. Nelson, D. Leong, L. Berhane, P. Hajdu and F. Lopez-Linares, *Energy Fuels*, 2016, **30**, 3783–3790.
17 M. Rezaee, F. Khalilian, H. Khodaverdi and M. R. Pourjavid, *J. Water Chem. Technol.*, 2021, **43**, 139–144.
18 G. Ma, X. Duan and J. Sun, *Spectrochim. Acta Part B At. Spectrosc.*, 2018, **149**, 57–61.
19 V. Padilla, N. Serrano and J. M. Díaz-Cruz, *Chemosensors*, 2021, **9**, 94.
20 M. Soylak, T. Zorlu and F. Uzcan, *J. Food Compos. Anal.*, 2025, **143**, 107545.
21 B. H. Abdelmonem, L. T. Kamal, R. M. Elbaz, M. R. Khalifa and A. Abdelnaser, *Heliyon*, 2025, **11**, e41713.
22 H. Liu, H. Cui, Y. Wang, Z. Jiang, L. Lei and S. Wei, *Appl. Spectrosc.*, 2023, **77**, 131–139.
23 L. M. Costa, F. A. Borges, M. H. da Silva Cavalcanti, A. C. do Lago, C. R. T. Tarley, G. de Fátima Lima Martins and E. C. Figueiredo, *Anal. Chim. Acta*, 2023, **1251**, 340709.
24 A. Elik, H. U. Haq, G. Boczkaj, S. Fesliyan, Ö. Ablak and N. Altunay, *J. Food Compos. Anal.*, 2024, **125**, 105843.
25 N. Benabdallah, M. Hadj Youcef, H. Reffas and A. Bendraoua, *Sep. Sci. Technol.*, 2021, **56**, 2407–2425.
26 M. Atakol, H. Akbiyik, A. Atakol, V. Yildirim, S. Bakirdere and O. Atakol, *Anal. Lett.*, 2025, **58**, 2997–3010.
27 M. Soylak, H. E. H. Ahmed and O. Goktas, *Food Chem.*, 2024, **450**, 139351.
28 S. Yang, S. Jiang, K. Hu and X. Wen, *Microchem. J.*, 2020, **154**, 104542.
29 J. Georgin, D. S. P. Franco, L. Meili, A. Bonilla-Petriciolet, T. A. Kurniawan, G. Imanova, E. Demir and I. Ali, *Adv. Colloid Interface Sci.*, 2024, **324**, 103096.
30 I. Khan, K. Saeed and I. Khan, *Arab. J. Chem.*, 2019, **12**, 908–931.
31 C. G. P. Moraes, R. S. Matos, C. dos Santos, Ş. Ţălu, J. M. Attah-Baah, R. S. S. Junior, M. S. da Silva, M. V. S. Rezende, R. S. Silva and N. S. Ferreira, *Materials*, 2022, **15**, 6555.
32 P. Leverett, J. K. Reynolds, A. J. Roper and P. A. Williams, *Mineral. Mag.*, 2012, **76**, 891–902.
33 P. Nag, S. Banerjee, Y. Lee, A. Bumajdad, Y. Lee and P. S. Devi, *Inorg. Chem.*, 2012, **51**, 844–850.
34 Ş. Tokalıoğlu, S. T. Hosseini Moghaddam, Y. Yılmaz and Ş. Patat, *Microchem. J.*, 2023, **195**, 109515.
35 J. Zhong, R. K. Kankala, S.-B. Wang and A.-Z. Chen, *Polymers*, 2019, **11**, 1627.
36 Y. Huang and P. Ruiz, *Appl. Surf. Sci.*, 2006, **252**, 7849–7855.
37 M. Filella, N. Belzile and Y.-W. Chen, *Earth-Sci. Rev.*, 2002, **59**, 265–285.
38 Y. Sasaki, *Appl. Catal., A*, 2000, **194–195**, 497–505.
39 A. Y. Nikulin, E. A. Zvereva, V. B. Nalbandyan, I. L. Shukaev, A. I. Kurbakov, M. D. Kuchugura, G. V. Raganyan, Y. V. Popov, V. D. Ivanchenko and A. N. Vasiliev, *Dalton Trans.*, 2017, **46**, 6059–6068.
40 T. Tojo, Q. Zhang and F. Saito, *Powder Technol.*, 2008, **181**, 281–284.
41 G. Saydan Kanberoglu, E. Yilmaz and M. Soylak, *J. Iran. Chem. Soc.*, 2020, **17**, 1627–1634.
42 K. Köseoğlu, H. İ. Ulusoy, E. Yilmaz and M. Soylak, *J. Food Compos. Anal.*, 2020, **90**, 103482.
43 N. Jalbani and M. Soylak, *Talanta*, 2015, **131**, 361–365.
44 A. M. Hameed, *J. Umm Al-qura Univ. Appl. Sci.*, 2022, **8**, 57–68.
45 M. R. Afshar Mogaddam, S. Beiramzadeh, M. Nazari Koloujeh, A. Changizi Kecheklou, M. M. Daghi, M. A. Farajzadeh and M. Tuzen, in *Green Analytical Chemistry*, Elsevier, 2025, pp. 59–117.
46 N. Altunay, M. Tuzen, B. Hazer and A. Elik, *Food Chem.*, 2022, **393**, 133464.
47 N. Altunay, A. Elik, G. Sarp, E. Yılmaz and H. İ. Ulusoy, *Microchem. J.*, 2021, **170**, 106765.
48 F. Uzcan, A. H. Kori and M. Soylak, *J. Food Compos. Anal.*, 2024, **130**, 106166.
49 X. Wang, J. Chen, Y. Zhou, X. Liu, H. Yao and F. Ahmad, *Anal. Lett.*, 2015, **48**, 1787–1801.
50 B. Topuz, *Biol. Trace Elem. Res.*, 2020, **194**, 295–302.
51 M. H. Kojidi and A. Aliakbar, *Environ. Monit. Assess.*, 2019, **191**, 145.
52 H. E. H. Ahmed and M. Soylak, *J. Food Compos. Anal.*, 2023, **121**, 105396.
53 P. T. Anastas and J. C. Warner, *Green Chemistry*, Oxford University PressOxford, 2000.
54 A. Gałuszka, Z. M. Migaszewski, P. Konieczka and J. Namieśnik, *TrAC, Trends Anal. Chem.*, 2012, **37**, 61–72.